

ANOMALOUS COMPRESSION OF LOW DENSITY POLYURETHANE FOAM SUBJECT TO SHOCK LOADING

C.S. ALEXANDER, W.D. REINHART, D. PETERSON

Sandia National Laboratories, Albuquerque NM 87185

Summary - This work reports the results of new experimentation on shock loaded 0.087 g/cc polymeric methylene diphenyl diisocyanate (PMDI) foam. This extremely distended material is only about 7% the density of fully dense polyurethane and has a lower density than previously studied polyurethane foams. The data is presented alongside previously published work on higher density PMDI up to and including full density polyurethane. Results clearly indicate anomalous response in this material indicated by a reversal in the pressure – density compression curve. This response is believed to be due to reactive decomposition of the polymer which occurs more readily in distended materials due to increased temperatures behind the shock front.

INTRODUCTION

Polyurethane (PU) foams are widely used in engineering applications to provide structural support while insulating against shock and vibration. A wide variety of polyurethane materials are available with densities ranging from full density PU (1.26 g/cc) to extremely distended foams with densities less than 0.1 g/cc. This family of materials has been widely studied under shock loading to determine the mechanical response. Most studies have concentrated on foams within the density range 0.16 – 1.26 g/cc with only limited data available at lower densities. Marsh¹ reported fully dense and foamed PU (densities of 1.264, 0.321, 0.28, 0.159, and 0.09 g/cc) with explosively driven flyer plates using the flash gap technique to measure shock velocities in multiple samples. Dattelbaum² furthered this work studying PU foam (densities of 0.348, 0.489, 0.626, and 0.868 g/cc) with gun launched flyer plates using VISAR and PDV diagnostics to determine shock velocities. Several other researchers have measured similar foams using gun launched flyer plates and other techniques at relatively low velocities under 1.5 km/s³⁻⁵.

Here we consider the shock response of 0.087 g/cc polymeric methylene diphenyl diisocyanate (PMDI) foam. This material is extremely distended with a density only 7% that of fully dense PU. Such distended material will experience large volume compression under shock loading resulting in higher temperature states than with more dense foams. Under similar conditions, anomalous compression, defined by *decreasing* density with increasing pressure, has been observed in foamed W⁶, Cu, and Al⁷. Dattelbaum et. al observed anomalous response in PU foams under 50% theoretical density² however, previous studies of low density PU foam under 0.1 g/cc density were not compressed sufficiently to observe an anomalous response. In this work we have compressed low density PMDI foam to a maximum of 3.39 GPa and have observed the expected anomalous response.

EXPERIMENTAL DETAILS

Material Tested

The material used in this study, polymeric methylene diphenyl diisocyanate (PMDI), is a PU based foam. The samples were produced by preparing 4 lb/cu ft encapsulant foam in a closed vessel overpacked to 6 lb/cu ft. Foam was produced in billets 4 inches in diameter by 8 inches long. After curing, the foam was machined to the final test dimensions of 19 mm diameter by 4 mm thick. The average density of the foam samples was 0.087 g/cc with a standard deviation of 0.66 mg/cc indicating good uniformity across the sample set.

Experimental Configuration

Experiments were conducted at the Sandia National Laboratories STAR facility utilizing the two-stage, propellant driven light gas gun. Impactors consisted of flat plates of tantalum or, in one test, copper, nominally 24 mm in diameter mounted to the front of a Lexan projectile. The target configuration is illustrated in figure 1. PMDI foam samples, nominally 19 mm in diameter, were backed with polymethylmethacrylate (PMMA) buffers and windows. The buffer/window interface had a 12 μ m aluminum foil that served as a reflector for the optical diagnostics and the buffer prevented abrasion of the reflector by the foam. Previous work by Dattelbaum² using similar diagnostics observed a reduction in light reflected during testing. The effect was more pronounced as foam density was decreased. The buffers were used to prevent degradation of the optical diagnostic signal.

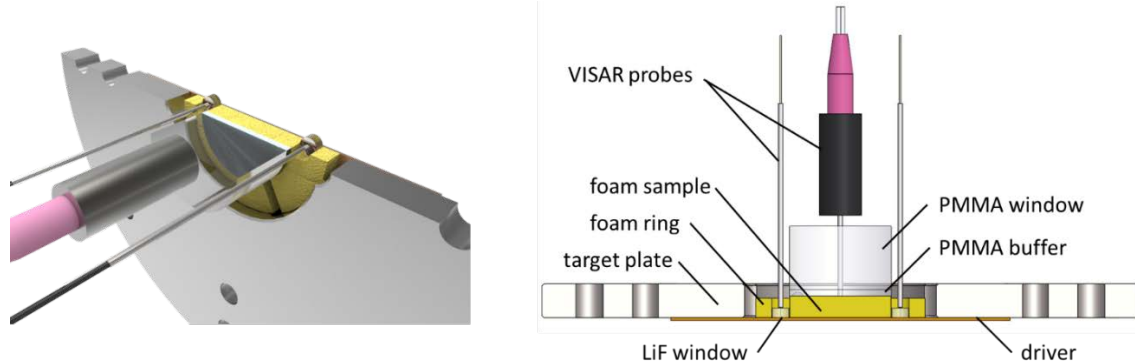


Figure 1: Experimental configuration.

VISAR⁸ diagnostics were used to measure the velocity of the window - buffer interface during the tests. A driver plate, nominally 75 mm in diameter, made of the same material as the impactor (Ta or Cu) was placed over the front of the foam target to prevent erosion of the foam by any potential ionized gas in front of the projectile. The foam target was mounted inside a foam ring (nominally 19mm ID x 40 mm OD) of similar material and thickness. This prevents higher velocity shock waves traveling in the aluminum target plate from affecting the one-dimensional loading on the foam sample. Additionally, this ring held four small lithium fluoride (LiF) windows (6 mm diameter by 3 mm thick) with front surface reflective coatings monitored with VISAR used to measure time of impact as well as impact tilt. Details of each part are listed in table I.

Table 1: Details of parts used in each experiment. Values shown are thicknesses in mm. Diameters were sufficient to ensure one-dimensional response. Materials used are shown in the column headings.

Shot ID	Impactor (Ta)	Driver (Ta)	Target (PMDI)	Buffer (PMMA)	Window (PMMA)
PMDI-2	2.040	1.030	4.080	1.210	11.800
PMDI-3	2.000	1.040	4.070	1.220	11.800
PMDI-4	3.993	0.493	3.914	1.229	11.830
PMDI-5	3.995	0.498	4.087	1.212	11.830
PMDI-6	4.272	0.505	4.044	1.214	11.820
PMDI-7	3.993*	0.528*	4.059	0.490	24.105

* The impactor and driver on shot PMDI-7 were copper.

Determination of the Shock Wave Speed

During each test, upon impact, a shock wave travels through the successive layers of the target (driver, sample, buffer, and window). Due to shock impedance mismatches at the interfaces (except the buffer window interface), wave reflection will occur. The effect will be to stepwise load or ring-up the foam sample to an ultimate steady state pressure. Each subsequent reverberation after the initial shock wave will further compress the foam sample. For the purposes of this study, only the initial wave is used. Subsequent reverberations probe the response of significantly compressed and heated foam which is not the focus of this work.

The primary measured quantity in these tests is the shock wave velocity (U_s) in the foam. This is measured by determining the shock transit time across the known sample thickness. The four LiF windows around the periphery of the foam target are used to determine the time when the shock wave enters the foam. The effect of impactor tilt is determined and included such that the time is measured at the center of the foam target. This is used in conjunction with the time the shock wave exits the sample at the foam - buffer interface.

Wave profiles are recorded at the window – buffer interface. Using the known Hugoniot response of PMMA^{9,10} and the measured *in-situ* particle velocity the shock wave speed in PMMA is determined. Combining this with the known buffer thickness results in the time for the shock to traverse the buffer. This is then removed resulting in the time for the shock wave to transit only the foam sample.

Determination of the Hugoniot State

Having measured the shock wave speed in the foam sample, the Hugoniot state is found by impedance matching with the known Hugoniot response of the impactor/driver material. This amounts to solving

the Rankine-Hugoniot equations¹¹ which describe materials subject to shock loading based on conservation of mass, momentum, and energy. These equations are:

$$(\text{mass}) \quad \rho_0 / \rho = 1 - u_p / U_s \quad (1)$$

$$(\text{momentum}) \quad \sigma = \rho_0 U_s u_p \quad (2)$$

$$(\text{energy}) \quad E = (\sigma / 2) (V_0 - V) \quad (3)$$

where ρ is the density, u_p is the particle velocity, U_s is the shock velocity, σ is the stress, E is the energy, and $V=1/\rho$. The zero subscripts denote the initial uncompressed state. In this form, the Rankine-Hugoniot equations describe a material shock loaded from an ambient state. This is a system of three equations with five unknown quantities. Thus by measuring any two of the unknowns, the remaining quantities are determined.

From equation 2, the foam sample is known to have been compressed along a Rayleigh line with slope ρ_0 / U_s . A similar equation holds for the impactor/driver material except u_p is replaced with $(u_p - V_i)$ where V_i is the impact velocity. This change is a result of the impactor being in motion at the time of impact. The intersection of the target Rayleigh line and the impactor/driver Hugoniot is the only state that mutually satisfies the Rankine-Hugoniot equations for both materials and thus determines the stress and particle velocity corresponding to the Hugoniot state. Using equation 1, the compressed density of each material is determined as well.

As mentioned earlier, only the first wave passing through the foam target is used to determine the Hugoniot state. Subsequent states could be analyzed using a slightly more complicated form of equations 1-3. However, due to compounding experimental errors which lead to greater uncertainty and the limited utility of such off-Hugoniot data, this analysis was not performed.

EXPERIMENTAL RESULTS

A series of six shots was conducted with PMDI foam targets as described previously. Recorded wave profiles are shown in figure 2. Not shown are wave profiles from shots PMDI-3 which was very nearly duplicated by PMDI-6 but with a thicker impactor and PMDI-7 which used a copper impactor and resulted in a slightly lower pressure than PMDI-6. Only the first few reverberations through the foam are shown. All subsequent analysis used only the initial shock wave passing through the foam. The times shown in the figure have been adjusted to represent shock wave timing through the foam. Time zero defines the shock break out from the driver plate. The time delay which occurred when the shock traveled through the PMMA buffer has also been subtracted. This time was determined from the measured *in-situ* PMMA particle velocity by using the PMMA equation of state⁹ to find the shock velocity. The transit time, dt , is then found from $dt = h / U_s$ where h is the PMMA buffer thickness. Thus, times shown for each shock wave arrival can be used to directly determine the shock wave velocity in the foam target according to $U_s = h/t$ where h is the thickness of the foam and t is from figure 2. Results are tabulated in table II.

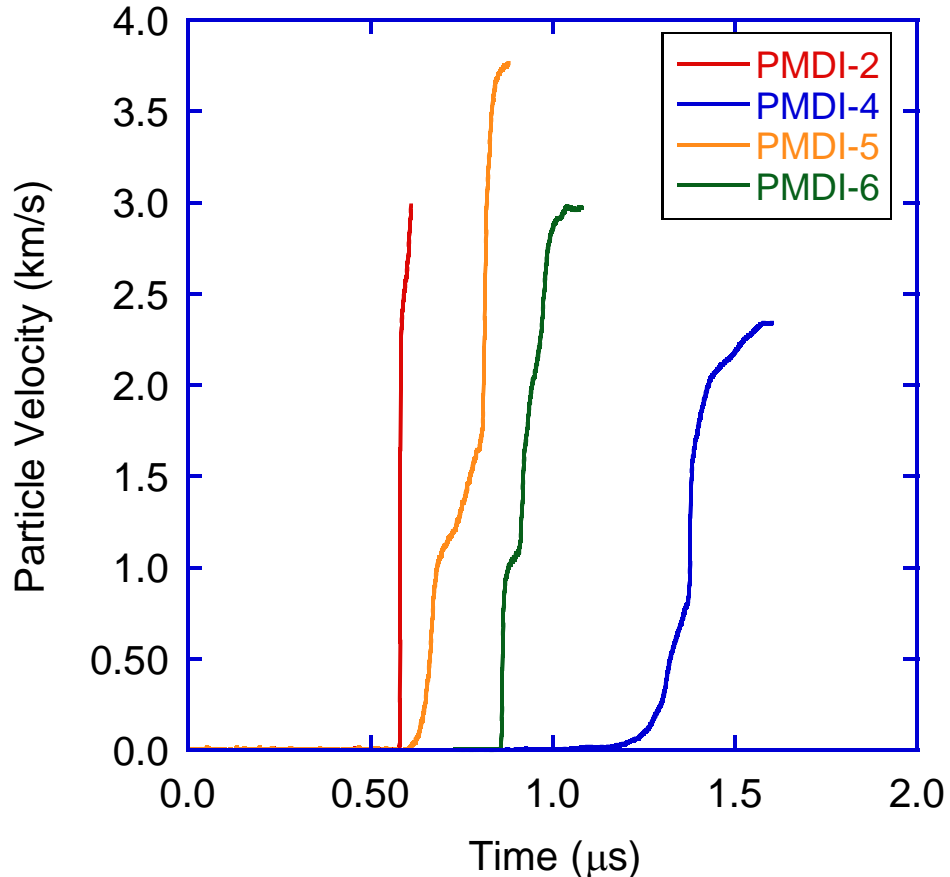


Figure 2: Experimental wave profiles. Note that PMDI-3 and PMDI-7 are not shown for clarity as they are similar to PMDI-6.

Table 2: Experimental parameters and results.

Shot ID	Impact Velocity (km/s)	Shock Velocity (km/s)	Particle Velocity (km/s)	Stress (GPa)	Initial Density (g/cc)	Compressed Density (g/cc)
PMDI-2	5.601	7.040	5.550	3.390	0.0878	0.415
PMDI-3	3.481	4.580	3.460	1.350	0.0866	0.354
PMDI-4	2.415	2.851	2.408	0.576	0.0863	0.554
PMDI-5	4.346	5.600	4.308	2.229	0.0868	0.376
PMDI-6	3.318	4.179	3.289	1.658	0.0858	0.403
PMDI-7	3.573	5.034	3.527	1.539	0.0867	0.290

Using the measured shock wave speed and the initial (uncompressed) foam density, a Rayleigh line was constructed and impedance matching performed to determine the Hugoniot state in the foam following the passage of the first wave. This process is illustrated graphically in figure 3 using data from shot PMDI-5. The equations of state used for Ta and Cu come from the LASL shock handbook¹. All tests were analyzed similarly. Again, results are tabulated in table II.

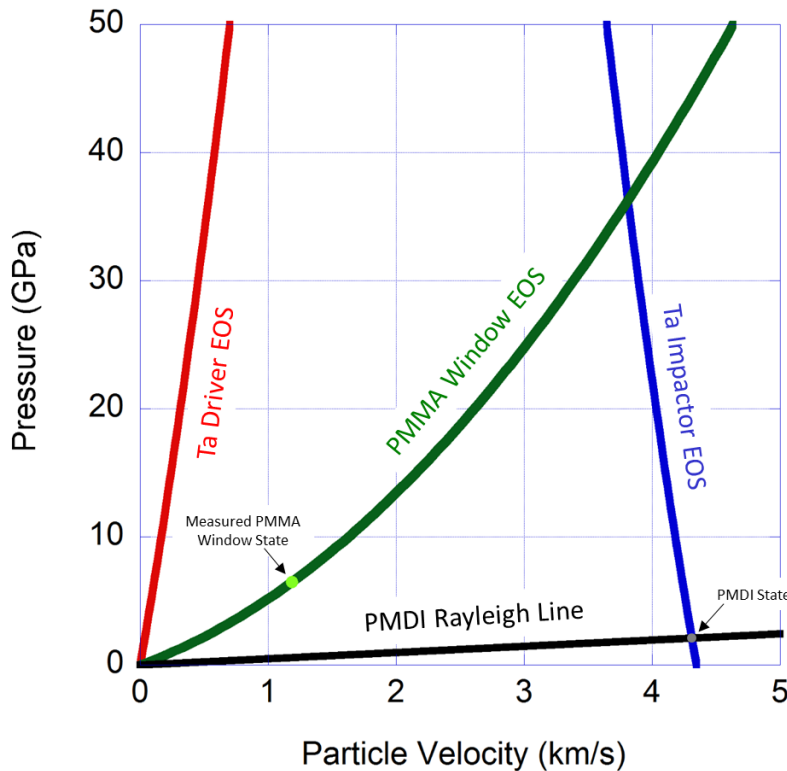


Figure 3: P-u diagram for shot PMDI-5.

Equation 1 was used to calculate the compressed density of the PMDI foam from the initial density and the measured shock and particle velocities. Results are also listed in table II. One will notice that the shock wave results in compression of the foam from 7% to 24-44% of fully dense PU.

DISCUSSION

The data in table II is shown graphically in figures 4 and 5 in the shock velocity – particle velocity and pressure – density planes respectively. Also shown are published data on similar but higher density foam reported by Marsh¹ and Dattelbaum². Data collected in this study is indicated by solid points while previously published data are open points. It is important to note that the previous studies included data on foams of several initial densities. In figures 4 and 5 there is no distinction drawn to the initial density of each datum. The reader is directed to the original publications for that level of detail. What is

important to consider in this work are the trends as initial density was decreased as the foam studied in this work was of lower initial density than any studied in the previous works.

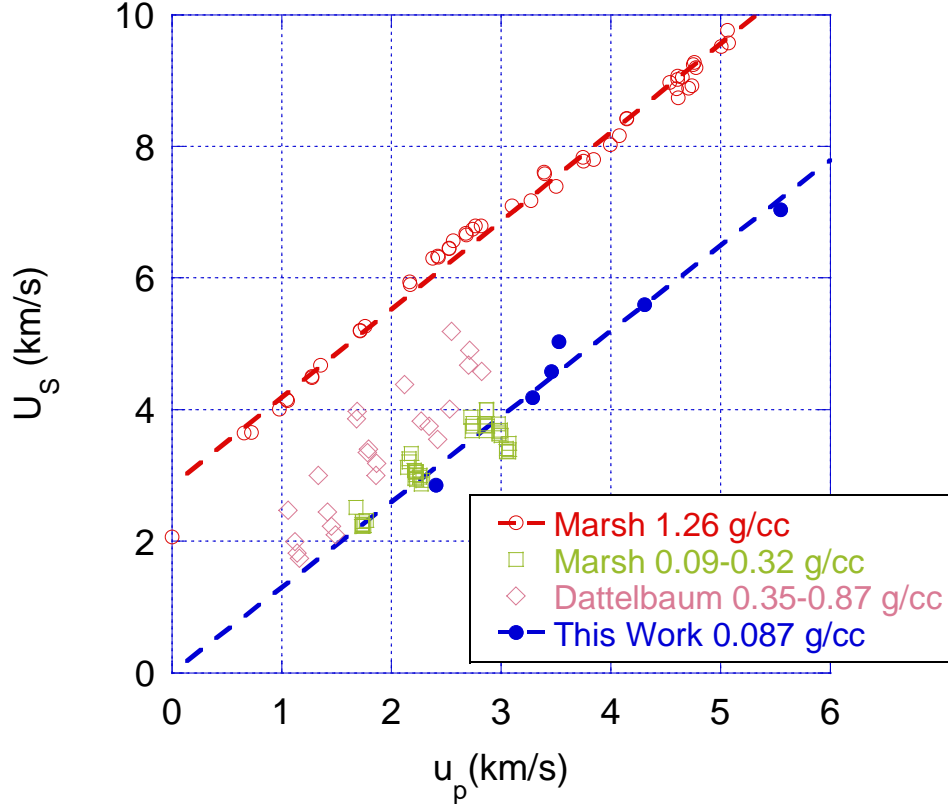


Figure 4: Experimental results shown in the shock velocity - particle velocity plane. New data on low density PMDI is shown in blue. Previous results from Marsh¹ and Dattelbaum² are shown for comparison. Dashed curves are linear fits to the data for this work and fully dense PU.

Considering figure 4, it is clear that the new data are represented by a linear relationship ($U_s = C_o + S u_p$) in shock velocity – particle velocity space. This is typical of most materials and was observed in the higher density foams as well. A fit to the current study data resulted in C_o of 9.4 km/s and S of 1.30. Of particular note is the fact that the 0.087 g/cc foam response closely matches that of 0.09 – 0.32 g/cc foam studied by Marsh and the 0.35 g/cc foam reported by Dattelbaum. The data of Dattelbaum indicated a trend of similar S with decreasing C_o parameters as the initial foam density was decreased. The data of Marsh for fully dense PU is also shown in the figure for reference. It appears that for densities below about 0.35 g/cc all PMDI foam can be fairly well represented by a single equation of state.

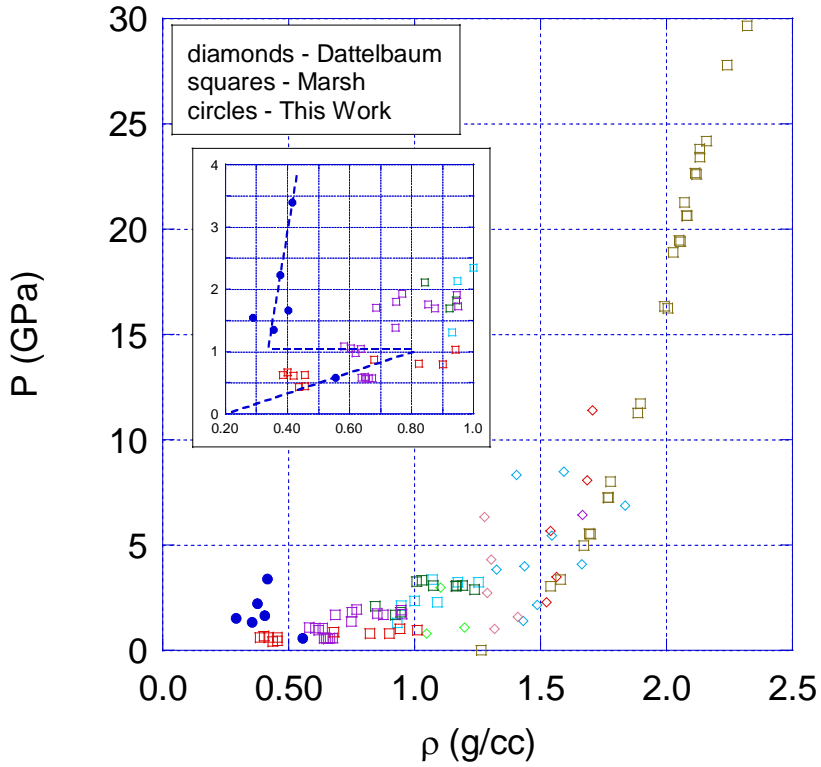


Figure 5: Experimental results shown in the pressure - density plane. New data on low density PMDI is shown as blue circles. Previous results (open symbols) from Marsh¹ (squares) and Dattelbaum² (diamonds) are shown for comparison. The inset shows an expanded view of the low pressure – density region where anomalous response is clearly seen in the new low density PMDI foam. The dashed curve is a guide to the eye illustrating the anomalous compression and not necessarily the exact path followed.

The data of figure 5 however illustrate a difference in the response of extremely low density foam. The figure shows the same data plotted in pressure – density space. The inset is an expansion of the low density region to show detail. In pressure – density space, the 0.087 g/cc foam is seen to initially follow a similar trend to the higher density foams as illustrated by the data point at about 0.55 g/cc. At slightly higher compression, the density of the foam is observed to decrease dramatically to around 0.3 g/cc. This path is illustrated in the inset by the dashed lines to help guide the eye. Note that the exact nature of the path is not known and additional testing in the transition region is required to understand the true path followed. This abrupt reduction in density with modest increase in pressure is the so-called anomalous response observed in low density foams and is an indication of reaction occurring due in part to the high temperatures present following compression of around six times in density. A dissociation of the polymer results in reaction products of much lower density. Shock loading to higher pressure states again shows densification of the reaction products. The data suggests that the reaction products will compress along a curve parallel to the full density PU although with limited data up to only 3.5 GPa this can not be confirmed at this time. Higher pressure states are difficult to obtain by the methods employed in this study due to the low shock impedance of the foam (and subsequent reaction products). Higher impact

velocities achievable by pulsed power or laser driven systems^{12,13} are required to achieve significantly higher pressures.

Dattelbaum reported similar evidence of anomalous compression. Those results clearly indicated a change to decreased density with increasing compression and suggested a return to compressive response with subsequent compression. However, the data on lower density foam (0.26 g/cc) was less convincing due to scatter in the results. The results presented here clearly show that anomalous compression response remains present in PMDI at lower initial densities. As noted by Dattelbaum, the data of Marsh was too scattered or insufficiently compressed to clearly show anomalous response.

CONCLUSION

New data on the dynamic response of low density PMDI foam has been reported. The foam was compressed to much higher pressure than previously reported for this material. The data clearly indicate an anomalous compression response wherein an abrupt reduction in density is observed with a modest increase in pressure. This type of response is an indication of a reaction occurring in the foam.

The anomalous response is an important consideration for modeling low density PMDI foam. While a linear U_s-u_p relation was still observed, the anomalous response leads to much lower densities at a given pressure when compared to fully dense PU. Further, there is a reduction in wave speed with decreasing initial density such that the C_0 term in a linear U_s-u_p relation needs to be reduced. It was observed however that 0.087 g/cc foam exhibits similar response to other foams up to about 0.35 g/cc.

ACKNOWLEDGEMENTS

The authors wish to thank Melissa Soehnel at Sandia National Laboratories for producing the foam studied. We also thank Tom Thornhill, John Martinez, Robert Palomino, and Heidi Anderson at the Sandia National Laboratories STAR facility for their assistance conducting the tests described in this work.

Sandia National Laboratories is a multi-mission laboratory operated by Sandia Corporation, a wholly owned subsidiary of Lockheed Martin Company, for the U.S. Department of Energy's National Nuclear Security Administration under contract DE-AC04-94AL85000.

REFERENCES

- ¹ S. P. Marsh, *LASL Shock Hugoniot Data* (University of California Press, Berkeley, 1980).
- ² D. M. Dattelbaum, J. D. Coe, C. B. Kiyanda, R. L. Gustavsen, and B. M. Patterson, *Journal of Applied Physics* **115** (2014).
- ³ B. W. Skews, *Shock Waves* **1**, 205.
- ⁴ M. E. Kipp, L. C. Chhabildas, W. D. Reinhart, and M. K. Wong, *AIP Conference Proceedings* **505**, 313 (2000).
- ⁵ J. R. Maw and N. J. Whitworth, *AIP Conference Proceedings* **429**, 111 (1998).
- ⁶ K. K. Krupnikov, M. I. Brazhnik, and V. P. Krupnikova, *Soviet Physics Jetp-Ussr* **15**, 470 (1962).

7 S. B. Kormer, A. I. Funtikov, V. D. Urlin, and A. N. Kolesnikova, Soviet Physics Jete-Ussr **15**, 477 (1962).

8 L. M. Barker and R. E. Hollenbach, Journal of Applied Physics **43**, 4669 (1972).

9 L. M. Barker and R. E. Hollenbach, Journal of Applied Physics **41**, 4208 (1970).

10 K. W. Schuler and J. W. Nunziato, Rheol. Acta **13**, 265 (1974).

11 I. A. B. Zel'dovich and I. U. P. Raizer, *Physics of shock waves and high-temperature hydrodynamic phenomena* (Dover Publications, Mineola, N.Y., 2002).

12 R. W. Lemke, M. D. Knudson, D. E. Bliss, K. Cochrane, J. P. Davis, A. A. Giunta, H. C. Harjes, and S. A. Slutz, Journal of Applied Physics **98**, 73530 (2005).

13 N. Ozaki, M. Koenig, A. Benuzzi-Mounaix, T. Vinci, A. Ravasio, M. Esposito, S. Lepape, E. Henry, G. Huser, K. A. Tanaka, W. Nazarov, K. Nagai, and M. Yoshida, Journal De Physique Iv **133**, 1101 (2006).